Functional Nanocavity Arrays via Amphiphilic Block Copolymer Thin Films

Andrew C. Miller,[†] Ryan D. Bennett,[†] Paula T. Hammond,[†] Darrell J. Irvine,[‡,§] and Robert E. Cohen*[,†]

Department of Chemical Engineering, Department of Materials Science and Engineering, and Department of Biological Engineering, Massachusetts Institute of Technology, 77 Massachusetts Avenue, Cambridge, Massachusetts 02139

Received August 28, 2007; Revised Manuscript Received November 29, 2007

ABSTRACT: The amphiphilic block copolymer polystyrene-*block*-poly(acrylic acid) (PS-*b*-PAA) forms micelles in toluene that can be cast onto a planar substrate to create quasi-hexagonal arrays of spherical PAA domains in a PS matrix. Treatment of these ultrathin films with an appropriate selective solvent swells the PAA domains and fractures open (cavitates) the PS matrix, thereby exposing the PAA chains to solution. Here we have investigated the conditions required for this cavitation process to occur and the end-state polymer morphology of close-packed films of PS-*b*-PAA micelles following treatment with a series of short alkyl chain alcohols or aqueous solutions of varying pH and ionic strength. Atomic force microscopy (AFM) and transmission electron microscopy (TEM) were employed to characterize the morphologies of the precursor and solvent-treated films. In addition to the effects of solvent conditions, we show that the cavitation process is influenced by the molecular weight of the PS block and is thermally reversible. Following cavitation, the nanopatterned regions of exposed PAA are available for conjugation chemistry, demonstrated here through selective linking of a fluorescently labeled protein.

Introduction

Block copolymers have been the subject of significant recent research due to their ability to self-assemble on the nanometer length scale into a variety of morphologies. Often, block copolymer films are solvent cast and annealed to form highly ordered equilibrium morphologies. A different approach can be utilized for block copolymers in selective solvents, which facilitate the formation of stable ordered structures in solution. The exchange of block copolymer molecules between micelles and solution is very slow compared to the exchange kinetics observed for low molecular weight surfactant micelles.[1] A favorable result of these slow exchange kinetics is the ability to retain a micellar morphology during casting from selective solvents onto solid substrates; this morphology becomes kinetically trapped in the final thin film upon solvent evaporation, even in cases for which the copolymer composition would suggest a transition to a different equilibrium heterogeneous phase. One of the most extensively studied polymer systems for formation of such micellar thin films is poly(styrene-*block*-*X*-vinylpyridine) (PS-*b*-P*X*VP) ($X = 2$ or 4). These films have been studied for their potential use in a variety of applications including data storage,[2] nanolithography,[3−11] and deposition of metal nanoparticle arrays such as gold catalyst particle arrays for zinc oxide nanowire synthesis,[12] iron oxide nanoparticles for carbon nanotube synthesis[13] and magnetic applications,[14] zinc oxide nanoparticles for optical devices,[15] and nickel[16] or gold[17−19] arrays for protein binding.

There has also been recent interest in the swelling and rearrangement of amphiphilic block copolymers for the creation of nanostructured films that contain nanopores and nanocavities. Previous work in our lab demonstrated the creation of 2-D arrays of nanocavities in polystyrene-*block*-poly(acrylic acid) (PS-*b*-PAA) thin films.[20] A PS-*b*-PAA polymer with PS and PAA block molecular weights of $M_n = 16\,400$ g/mol and $M_n = 4500$ g/mol, respectively, formed kinetically trapped spherical inverse micelles in toluene after a suitable heating and cooling cycle described earlier,[20] which were then spin-cast onto a planar substrate to create a quasi-hexagonal array of PS-*b*-PAA micelles. When films of PS-*b*-PAA were exposed to highly alkaline aqueous solutions with monovalent cations, the PAA domains swelled and ruptured the glassy PS corona, a process we termed cavitation. We have also shown control over the size and spacing of the spherical PAA domains of these micellar films by varying the molecular weight of the block copolymer and by adding PS homopolymer to the block copolymer micellar solutions before casting films.[21] The ability to pattern these nanostructured films using soft lithographic techniques was also demonstrated.[22] A variety of multivalent metal ions have been loaded into these micelles pre- and postcavitation. If the polymer is subsequently plasma-etched or pyrolized, a 2-D array of inorganic nanoparticles is produced on the supporting substrate, which, for the particular case of iron oxide, we have used successfully as a structured catalyst for carbon nanotube synthesis.[22−24]

A number of studies have characterized the formation of nanocavities in related polymer systems. Cong et al.[25] and Li et al.[26] have observed similar cavitation behavior for films of PS-*b*-P2VP micelles when these films were exposed to high relative humidity or acetic acid, respectively. Semifluorinated alkanes can form arrays of nanocavities,[27] but the surfaces of such films consist of only a single functionality, unlike some of the block copolymer systems that contain two distinct, patterned functionalities. PS-*b*-P2VP dissolved in THF along with 1,5-dihydroxynaphthalene (DHN) were cast into films of P2VP cylinders aligned perpendicular to the substrate.[28] Methanol treatment of the film removes the DHN from the cylinders leading to the creation of nanoporous films. PS-*b*-PMMA

* To whom correspondence should be addressed. E-mail: recohen@mit.edu.
[†] Department of Chemical Engineering.
[‡] Department of Materials Science and Engineering.
[§] Biological Engineering Division.

10.1021/ma7019418 CCC: $40.75
Published on Web 02/16/2008

cylinders have also been used to create nanoporous films[29,30] by irradiating the film and then rinsing away the degraded PMMA. Xu et al.[31,32] have studied the reversible swelling of PAA cylinders aligned perpendicular to the surface in a PS matrix. The oriented cylinders form cavities or mushrooms depending on the pH of the swelling solution.

Here we have focused on characterizing the cavitation phenomenon of micellar thin films as a function of solvent treatment, using PS-*b*-PAA as a model system. We exposed micellar films of various molecular weights to aqueous solutions with a range of pH and ionic strengths as well as to alkyl alcohols of varying chain length and characterized the resulting film morphologies via atomic force microscopy (AFM). The cavitation process can be reversed by thermally annealing the films. We also visualized the rearrangement of the PAA chains following solvent treatment using transmission electron microscopy (TEM) and demonstrated the availability of the micellar core PAA blocks for participation in postcavitation conjugation chemistry.

Experimental Section

Materials. Three poly(styrene-*block*-acrylic acid) diblock copolymers (PS-*b*-PAA) were used in this work with the following molecular weights and nomenclature: PS-*b*-PAA 16.4-*b*-4.5 (M_n(PS) = 16 400 g/mol, M_n(PAA) = 4500 g/mol, PDI = 1.05), PS-*b*-PAA 42-*b*-4.5 (M_n(PS) = 42 000 g/mol, M_n(PAA) = 4500 g/mol, PDI = 1.15), and PS-*b*-PAA 66.5-*b*-4.5 (M_n(PS) = 66 500 g/mol, M_n(PAA) = 4500 g/mol, PDI = 1.07). These copolymers, along with their molecular-level characterization data, were purchased from Polymer Source, Inc. Toluene (HPLC grade, 99.8%), *n*-propanol, Tween 20, and lead(II) acetate trihydrate ($PbAc_2$) were obtained from Sigma-Aldrich Co. Methanol, ethanol, isopropanol, *n*-butanol, *n*-octanol, hydrochloric acid (37%), sodium chloride, and sodium hydroxide were purchased from Mallinckrodt Chemicals. Phosphate buffered saline (PBS) was obtained from VWR international. EZ-link amine-PEO-biotin and EDC were purchased from Pierce Biotechnology. Streptavidin, Alexa Fluor 647 conjugate was purchased from Molecular Probes. Poly(acrylic acid) (PAA) (M_n = 90 000, 25% aqueous solution), sulfonated polystyrene (SPS) ($M_n \sim 70\,000$), and poly(allylamine hydrochloride) (PAH) (M_n = 70 000) were purchased from Polysciences. All chemicals were used as received. Silicon nitride TEM membrane window substrates were purchased from Structure Probe, Inc. Each substrate (surface area ~ 4.5 mm^2) consisted of a 100 nm thick amorphous, low-stress Si_3N_4 membrane supported on a 0.2 mm thick silicon wafer that was back-etched in the center to create the electron transparent Si_3N_4 window (surface area ~ 0.2 mm^2). All aqueous solutions were made using deionized water (>18 MΩ cm, Millipore Milli-Q).

Microscopy. TEM was performed on a JEOL 2000FX operating at 200 kV. AFM was performed on a Digital Instruments Dimension 3000 Nanoscope IIIA scanning probe microscope using a silicon RTESP cantilever from Veeco Instruments operating in tapping mode. Fluorescence images were obtained using a Zeiss Axiovert 200 microscope equipped with a Roper Scientific CoolSnap HQ CCD Camera.

Sample Preparation. Each of the three different molecular weights of PS-*b*-PAA (listed in the Materials section) was separately mixed with toluene at 25C at a concentration of 10 mg/mL: all of the resulting solutions were slightly cloudy. Solutions of the PS-b-PAA 16.4-*b*-4.5 were heated to 140 °C for 20 min and allowed to cool in air to room temperature, which results in a change from cylindrical to spherical block copolymer micelles.[20] The other PS-*b*-PAA molecular weights formed spherical micelles at room temperature. Thin films (25−200 nm) were then created by spin-casting the micellar solutions onto glass, silicon, or silicon nitride substrates at spin rates of 1600−8000 rpm. The use of electron transparent silicon nitride window grids allows TEM characterization while providing a flat substrate on which films were spin-cast. In order to prevent film delamination experienced when incubating a hydrophobic film on a hydrophilic substrate in a polar solvent, a polyelectrolyte multilayer adhesion layer on a glass substrate was used for some experiments. The polyelectrolyte multilayer film consisted of five bilayers of poly(allylamine hydrochloride) (PAH) dipped at a concentration of 10 mM on a repeat unit basis at pH 3.5 with 0.1 M NaCl and sulfonated polystyrene (SPS) at a concentration of 10 mM on a repeat unit basis at pH 3.5 with 0.1 M NaCl. A film consisting of three and a half bilayers of PAH dipped at pH 7.5 and a concentration of 10 mM on a repeat unit basis and poly(acrylic acid) dipped at pH 3.5 at a concentration of 10 mM on a repeat unit basis was then deposited on top. This results in a film with a PAH top layer and a water advancing contact angle of 70°, as described elsewhere.[33]

The resulting thin film morphology is spherical PAA domains quasi-hexagonally arranged in a PS matrix.[20] For TEM imaging, films were immersed in a saturated lead(II) acetate trihydrate solution for 24 h to load lead ions into the PAA domains. The lead ions diffuse through the polystyrene corona and bind to the carboxylic acids of the PAA domains. Cavitation is suppressed because the divalent lead ions ionically cross-link the neutralized PAA cores and prevent swelling. This absence of cavitation behavior was also observed in earlier work when di-or trivalent cations were employed.[20]

For cavitation, film-coated substrates were placed in 20−30 mL of the selected solution for varying amounts of time and dried under vacuum overnight at 25 °C prior to AFM imaging. Films treated in PBS buffer or solutions pH adjusted with NaOH were rinsed with deionized water prior to drying under vacuum. This rinsing procedure eliminated any precipitated salt on the surface, facilitating AFM imaging of the polymer structure. Nanocavity size was determined by performing section analysis of AFM images using NanoScope Software v5.30. Taking section lines directly through cavities allowed their size to be determined. 50 cavities were analyzed per image to determine nanocavity size and distribution.

The procedure used for coupling the amine−PEO−biotin linker and streptavidin−Alexa Fluor 647 is described elsewhere.[34] Briefly, films were incubated in 0.5 μg/mL EZ link amine−PEO−biotin linker molecule, 5 mg/mL EDC in Milli-Q water for 4 h at room temperature. Films were washed five times with Milli-Q water and then incubated for 30 min at room temperature in PBS buffer at pH 7.4 with 0.5 μg/mL streptavidin−Alexa Fluor 647 conjugate and 0.1% v/v Tween 20. Films were then washed five times in PBS.

Results and Discussion

In previous work,[20] we found that inverse spherical PS-*b*-PAA micelles formed in toluene and cast as close-packed micellar films on solid substrates reorganized upon exposure to alkaline aqueous NaOH solutions. This cavitation process was driven by water swelling of the hydrophilic PAA blocks in the cores of the micelles, and led to fracture of the glassy polystyrene corona at the free surface of the film. To further investigate this reorganization phenomenon, we first examined the role of solvent quality on micelle cavitation. Micellar films were exposed to a series of alkyl alcohols of varying chain length, to allow a continuous variation of the selectivity of the solvent toward each block (Table 1).

Films of PS-*b*-PAA 16.4-*b*-4.5 micelles cavitated when incubated in methanol, ethanol, *n*-propanol, or isopropanol. In contrast, the micelles did not cavitate, maintaining their as-cast morphology, when exposed to *n*-butanol or *n*-octanol. These results are illustrated by the AFM images in Figure 1, which show an as-cast micellar film (A) and the results of treating films of PS-*b*-PAA 16.4-*b*-4.5 with isopropanol (B) or *n*-butanol (C) for 30 min and then drying under vacuum overnight. Extended treatment times (up to 192 h) produced the same morphologies seen following 30 min treatment times across all samples. While it is likely that the PAA domains swelled to

Table 1. Solubility Parameters of Solvents Used in Micellar Assembly and Film Treatments

solvent	cavitation observed	solubility parameter, δ $(cal/cm^3)^{0.5}$
water	yes	23.4
methanol	yes	14.5
ethanol	yes	12.7
n-propanol	yes	11.9
isopropanol	yes	11.5
n-butanol	no	11.4
n-octanol	no	10.3
toluene	N/A	8.9
acrylic acid	N/A	12.0
styrene	N/A	9.3

some degree in *n*-butanol and *n*-octanol, this swelling was not significant enough to cause rupture of the glassy PS domains. It is also possible that the solvent could plasticize the PS block such that its increased flexibility led to swelling or stretching rather than cavitation; however, Yaffe and Kramer[35] have shown that when soaked in *n*-butanol, the T_g of PS decreases from 100 °C to 71 °C and when soaked in *n*-propanol, the T_g is depressed to 81 °C. These T_g values are still well above room temperature. From this fact, we conclude that the effect on the PS caps of exposure to solvent does not play a significant role in the suppression of cavitation in *n*-butanol-treated films, and the change in cavitation behavior between isopropanol and *n*-butanol must be due to differences in PAA swelling. These results illustrate that the polarity of the solvent plays a major role in the swelling and cavitation of the PAA domains, as the alcohols represent a homologous series of polar molecules with systematically variable polarity and hydrophobicity.

Next, we examined the effect of varying the solvent interaction with the PAA blocks by exposing micellar films to aqueous solutions of varying pH and ionic strength. Because PAA is a weak polyacid, the charge along the polymer backbone increases with increasing pH. This charging phenomenon drives the polymer chain to a more extended conformation in order to minimize the electrostatic interactions between neighboring repeat units along the chain. We thus expect swelling of the interior PAA block of the micelle and cavitation to be favored as pH increases.

The morphology of cavitated PS-*b*-PAA 16.4-*b*-4.5 polymer films and the degree to which the micelle opens depend on pH, as seen in the AFM images in Figure 2 for the case of films treated for 30 min in aqueous solutions ranging in pH from 2.0 to 11.6 at low ionic strength. For treatment in pH 2.0 HCl (ionic strength, $I = 10$ mM), seen in Figure 2A, only a very subtle depression can be seen on the top of the micelles, suggesting that a morphological rearrangement has occurred but to a much lower degree than in the films treated at higher pH. In comparison, films treated with pH 5.6 deionized water exhibited easily distinguishable cavities, and the PS corona of each micelle was fractured. This fracture and rearrangement was even more evident for the film treated in pH 7.4 NaOH ($I = 3$ μM). In the film treated in pH 11.6 NaOH ($I = 4$ mM), film rearrangement resulted in a morphology that was significantly different from the other films studied. In films treated in pH 2.0−7.4 the boundaries between adjacent micelles remains defined, but for pH 11.6 treated films the boundaries are difficult to determine, and with the exception of the hexagonal arrangement, it has almost completely lost is resemblance to the as-cast films. Figure 2E shows the cavity diameter for PS-*b*-PAA 16.4-*b*-4.5 films treated in pH 5.6 deionized water, pH 7.4 NaOH and pH 11.6 NaOH, as determined from analyzing the AFM data. These values are only approximate due to the comparable size of the cavities and the AFM tip; however, a clear trend of increasing cavity diameter with increasing pH of the solution is observed. This is consistent with the increased swelling of PAA with increasing pH. PAA domain swelling and chain stretching mechanisms have been show to create topologically similar structures in uncapped PAA cylinders aligned perpendicular to the surface in PS-*b*-PAA thin films.[32] Cavitation of micelle films at one pH followed by exposure of the film to a second aqueous solution with a higher pH than the initial solution led to a morphology identical to that resulting from a single treatment in the higher pH solution. The PAA chains swell more when exposed to the higher pH solution and thus further cavitate the PS caps compared to their state after the first solution treatment at a lower pH. However, sequential exposure of a film to a higher pH followed by a lower pH left the film in the higher pH cavitated structure, presumably because the PAA chains already have ample solution volume available to them to swell.

Ionic strength, like pH, plays a role in the swelling of polyelectrolyte brushes, hydrogels, and other polyelectrolyte films. For many weak polyelectrolyte systems, increasing the ionic strength of the solution leads to a decrease in the swelling of films. However, for weak polyelectrolyte brushes, including poly(acrylic acid), the opposite behavior has been predicted[36−41] and observed[42,43] at low ionic strengths. For PAA specifically, brush swelling has been predicted and observed to be greater for ionic strengths approaching 1 M compared to the swelling at <1 mM at constant pH.[39] This behavior is determined by two opposing effects as the ionic strength increases. The first is a decrease in the electrostatic potential (increased ionic screening), which would decrease the swelling of the brush. The second is the charge state of the polymer itself. For a weak polyacid, as the ionic strength of the solution is increased, the pK_a of the polymer is shifted to a lower pH and the charge of the polymer increases. This charging of the polymer chain and accumulation of associated counterions in the PAA domain leads to a higher intrabrush osmotic pressure and increased brush swelling. It is this latter effect that dominates at low ionic strength for weak polyelectrolyte brushes and leads to increased swelling with increased ionic strength. We expected that a similar behavior could prevail in micellar films, as the PAA chains are in a brushlike state pinned at the PS−PAA domain boundary.

In order to investigate what effect ionic strength has on the swelling and cavitation behavior of PS-*b*-PAA micellar films, we treated 16.4-*b*-4.5 films in pH 7.4 phosphate buffered saline ($I = 150$ mM) (Figure 3). The morphology of the film more closely resembles that of the films treated in pH 11.6 NaOH ($I = 4$ mM) than the films treated in pH 7.4 NaOH ($I = 3$ μM). This is consistent with the behavior of weak polyelectrolyte brushes discussed above. By increasing the ionic strength of the solution while remaining in the low ionic strength regime as applicable to PAA, the swelling of the PAA domain increases, leading to a morphology that resembles a film treated at higher pH but lower ionic strength. Similar results were obtained for micelle films treated with pH 7.4 NaCl solutions of 10−150 mM (data not shown).

The reorganization of micellar films in response to aqueous solutions of varying pH demonstrates that selectively varying the interaction of the solvent with the core block of the micelles can substantially modulate the final structure of the cavitated films. However, the glassy PS corona of the micelles also plays a role in controlling cavitation behavior and morphology. By increasing the PS block length while holding the PAA block length constant, the PS:PAA ratio of the polymer increases. As

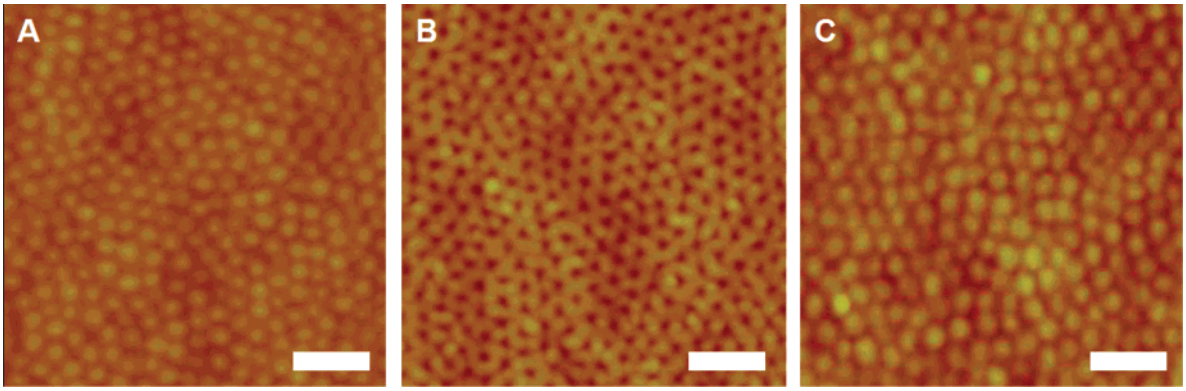

Figure 1. AFM height images of PS-*b*-PAA 16.4-*b*-4.5 films (A) as-cast and treated in (B) isopropanol and (C) *n*-butanol for 30 min. Scale bars are 100 nm and height scales are 20 nm.

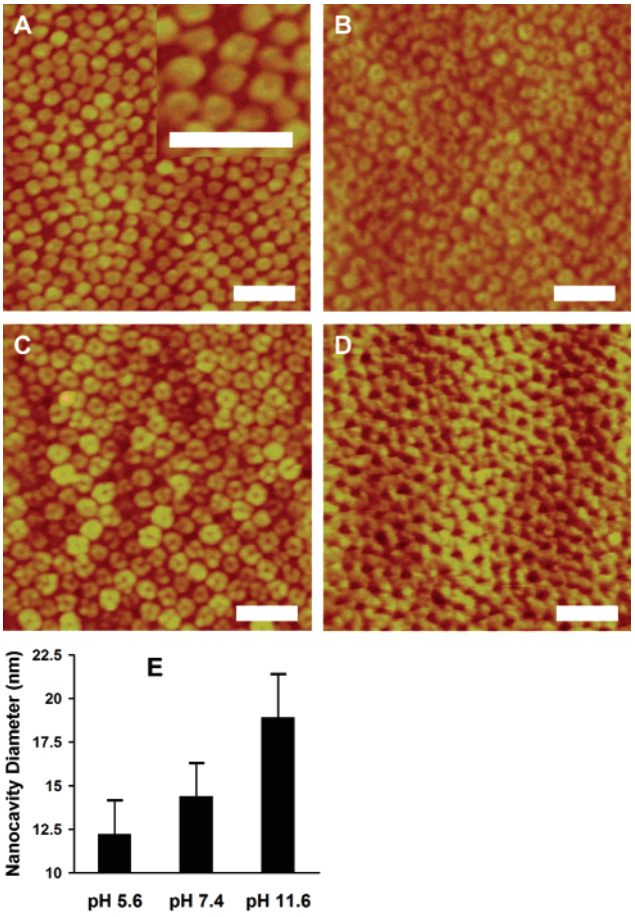

Figure 2. AFM height images of PS-*b*-PAA 16.4-*b*-4.5 films treated for 30 min in (A) pH 2.0 HCl, (B) MQ water pH 5.6, (C) pH 7.4 NaOH, and (D) pH 11.6 NaOH. Scale bars are 100 nm, and height scales are 20 nm. (E) Size of nanocavities resulting from described treatments for PS-*b*-PAA 16.4-*b*-4.5 determined from AFM images.

a consequence, for each PAA chain there is more PS present, and the swelling of the PAA chain required to fracture the PS caps will increase, and thus we expect the pH of the solution required to cavitate the micelle will be higher. In addition, the critical molecular weight for entanglement coupling in PS is about 36 kg/mol;[44] as a result, varying the PS block molecular weight around this value would be expected to produce significant changes in the polystyrene's ability to mechanically resist swelling of the encapsulated PAA core. To test this hypothesis, we examined the cavitation behavior of PS-*b*-PAA 42-*b*-4.5 and 66.5-*b*-4.5 micelles following exposure to aqueous solutions of varying pH (Figure 4). Unlike PS-*b*-PAA 16.4-*b*-4.5 micelles, PS-*b*-PAA 42-*b*-4.5 does not cavitate in pH 5.6 deionized water, even after long treatment times (up to 168 h). However, treating with a pH 7.4 NaOH solution triggered cavitation. When the PS block length increased to 66.5 kg/mol, the resulting micellar films did not cavitate in NaOH solution with a pH as high as 9.6 but did cavitate upon exposure to pH 11.6. At sufficiently large PS molecular weights, cavitation might be suppressed at all pH values.

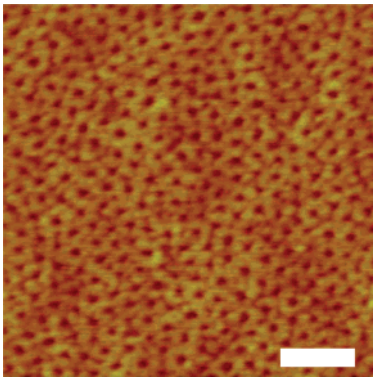

Figure 3. AFM height image of PS-*b*-PAA 16.4-*b*-4.5 film treated in PBS buffer (I = 150 mM) at pH 7.4 for 30 min. Scale bar is 100 nm, and height scale is 20 nm.

In order to further investigate the rearrangement of the polymer thin film upon exposure to aqueous solution, we examined the selective loading of multivalent metal ions into micelle films pre- and postcavitation. The TEM images in Figure 5 show a PS-*b*-PAA 16.4-*b*-4.5 films that has been exposed to aqueous 0.4 mM lead(II) acetate solution and a PS-*b*-PAA 16.4-*b*-4.5 film that was exposed to pH 11.6 NaOH and subsequently to an aqueous lead(II) acetate solution. AFM images (not shown) confirm that the film in Figure 5A has the familiar as-cast morphological topology (Figure 1A) of quasi-hexagonal closed-packed micelles and that the film in TEM image 5B exhibits the expected cavitated morphology (Figure 2). For the as-cast films, the lead staining yields a circle with small clusters visible inside the circular area of the micelle. The cavitated film exhibits a different staining pattern characterized by a ring structure. We believe this ring structure is a result of the cavitated morphology that leaves a cylinder-like cavity, the walls of which are covered with a PAA brush. This proposal is consistent with the observation in Figure 5B that the walls of the cylinder-like cavity appear dark with light staining in the center.

The results described above characterize the swelling of PAA domains leading to the fracture of the PS caps, creating arrays of nanocavities. To investigate whether the reverse process can occur (cavitated micelles returning to their as-cast spherical

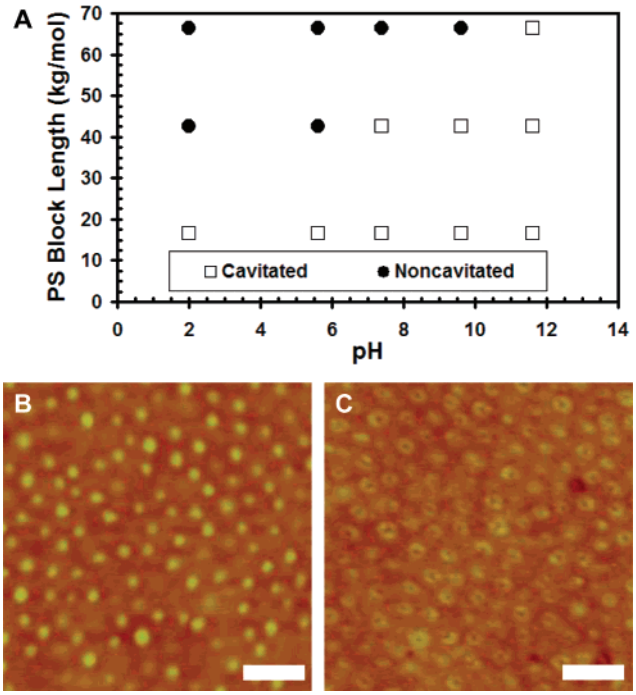

Figure 4. Cavitation behavior of PS-*b*-PAA with a PAA block of M_n = 4.5 kg/mol and changing PS block length for aqueous solution treatments of varying pH. AFM height images of PS-*b*-PAA 66.5-*b*-4.5 after a 30 min treatment in (B) pH 9.6 NaOH solution and (C) pH 11.6 NaOH solution. Scale bars are 100 nm, and height scales are 20 nm.

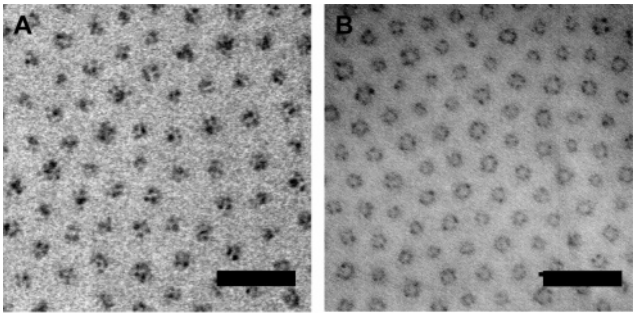

Figure 5. TEM images of PS-*b*-PAA 16.4-b-4.5 films stained with lead acetate. Image A is of as-cast film, and image B is a film that has been cavitated in pH 11.6 NaOH before staining. Scale bars are 100 nm.

morphology), we thermally annealed cavitated PS-*b*-PAA 16.4-*b*-4.5 thin films. The T_g of bulk PS is about 100 °C, so it is expected that the PS chains on the free surface of our ultrathin films would be sufficiently mobile during annealing at 100 °C. Micellar films that had first been treated in pH 7.4 NaOH and had the morphology of Figure 2C were thermally annealed at 100 °C for 24 h. After annealing, the films were imaged in AFM and the morphology had returned to that of the as-cast films as illustrated by Figure 1A (data not shown). Annealed films that had returned to this as-cast morphology, cavitated a second time upon treatment in pH 7.4 NaOH (I = 3 μM).

Cavitation of the PS caps and the resulting exposure of the PAA chains produces a nanopatterned surface of PS and PAA domains. EDC, a carbodiimide, zero-length cross-linking agent that couples primary amines and carboxylic acids, can then be utilized to selectively bind primary amine functionalized molecules to the exposed carboxylic acid moieties of the PAA domains of our cavitated films. This capability, combined with our previous work[21,22] that demonstrated control over the center-to-center spacing and PAA domains size of PS-*b*-PAA thin

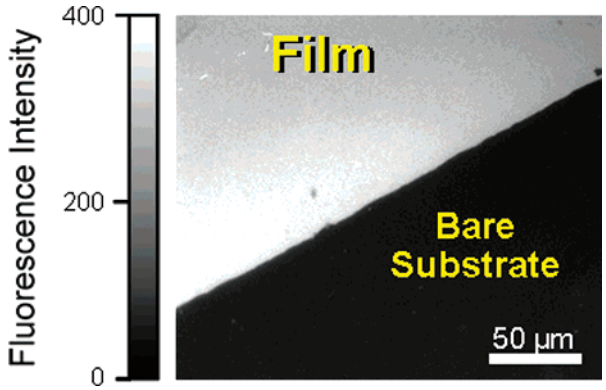

Figure 6. Fluorescence image demonstrating the specific coupling a streptavidin−Alexa Fluor conjugate to the carboxylic acid groups of a cavitated PS-*b*-PAA (16.4-*b*-4.5) film via a NH_2−triethylene glycol−biotin linker molecule. The substrate is a polyelectrolyte multilayer on glass as described in the Experimental Section. Expsoure time is 400 ms.

films, points to the potential to create controlled 2-D nanopatterned arrays of many different molecules. To demonstrate this concept, we have selectively bound a streptavidin−Alexa Fluor conjugate to a cavitated PS-*b*-PAA 16.4-*b*-4.5 film. First, a primary amine functionalized triethylene glycol biotin linker molecule was covalently linked to the surface using EDC chemistry, and then the film was incubated in a streptavidin−Alexa Fluor solution. These films were then imaged in a fluorescence microscope to confirm binding, as seen in Figure 6. The cavitated film in Figure 6 was treated with the complete coupling reaction followed by streptavidin binding. The strong fluorescence of the conjugated film confirms both the availability of the PAA groups to the solution and the ability to functionalize these nanocavities postcavitation. Control reactions were performed where no biotin linker molecule or no streptavidin−Alexa Fluor conjugate was present. The absence of fluorescence intensity in these films (data not shown) indicates that nonspecific binding of both the biotin linker molecule and the strepatvidin−Alexa Fluor to the cavitated micelles films was low.

Conclusions

AFM imaging was successful in capturing the morphological rearrangement of PS-*b*-PAA micellar thin films that were exposed to alcohols and aqueous solutions of varying pH and ionic strength. We have shown that solvent polarity, pH of the aqueous solution, and the ionic strength of the solution determine whether a micellar film of a given molecular weight and composition will cavitate and expose the PAA chains to film surface. The resulting cavity size is also dependent on these variables. The results support the contention that the cavitation behavior is a result of PAA domain swelling which induces fracture and rearrangement of the PS caps. At constant PAA block molecular weight, varying the molecular weight of the PS domains also affects cavitation behavior of the micelles. A higher pH solution is required to cavitated micelles with larger PS molecular weights. The cavitation process is thermally reversible; annealing films at a temperature near the T_g of the PS block returned the films to the original precavitated morphology. The morphological rearrangement was also visualized by TEM imaging of films selectively stained for PAA. We also demonstrated selective linking of a streptavidin−Alexa Fluor conjugate to the PAA chains of the cavitated micellar film. The success of this conjugation chemistry demonstrates the availability of the PAA domains to reagents in aqueous

solution and suggests the potential of the novel 2-D cavitated nanostructured system for biological applications.

Acknowledgment. This work was supported by The Institute for Soldier Nanotechnologies at MIT, Team 3.17, Contract DAAD19-02-D-0002, and the National Defense Science and Engineering Graduate Fellowship. This work made use of the Shared Experimental Facilities supported by the MRSEC Program of the National Science Foundation under Award DMR 02-13282.

References and Notes

(1) Moffitt, M.; Khougaz, K.; Eisenberg, A. *Acc. Chem. Res.* **1996**, *29*, 95−102.
(2) Terris, B. D.; Thomson, T. *J. Phys. D: Appl. Phys.* **2005**, *38*, R199−R222.
(3) Hamley, I. W. *Nanotechnology* **2003**, *14*, R39−R54.
(4) Harrison, C.; Park, M.; Chaikin, P. M.; Register, R. A.; Adamson, D. H. *J. Vac. Sci. Technol. B* **1998**, *16*, 544−552.
(5) Harrison, C. K.; Adamson, D. H.; Park, M.; Chaikin, P. M.; Register, R. A. *Abstr. Pap. Am. Chem. Soc.* **1997**, *214*, 116-Pmse.
(6) Park, M.; Harrison, C.; Chaikin, P. M.; Register, R. A.; Adamson, D. H. *Science* **1997**, *276*, 1401−1404.
(7) Harrison, C.; Park, M.; Chaikin, P.; Register, R. A. *Abstr. Pap. Am. Chem. Soc.* **1996**, *212*, 143-Poly.
(8) Glass, R.; Arnold, M.; Cavalcanti-Adam, E. A.; Blummel, J.; Haferkemper, C.; Dodd, C.; Spatz, J. P. *New J. Phys.* **2004**, *6*.
(9) Gorzolnik, B.; Mela, P.; Moeller, M. *Nanotechnology* **2006**, *17*, 5027−5032.
(10) Jung, J. M.; Kwon, K. Y.; Ha, T. H.; Chung, B. H.; Jung, H. T. *Small* **2006**, *2*, 1010−1015.
(11) Bratton, D.; Yang, D.; Dai, J. Y.; Ober, C. K. *Polym. Adv. Technol.* **2006**, *17*, 94−103.
(12) Haupt, M.; Ladenburger, A.; Sauer, R.; Thonke, K.; Glass, R.; Roos, W.; Spatz, J. P.; Rauscher, H.; Riethmuller, S.; Moller, M. *J. Appl. Phys.* **2003**, *93*, 6252−6257.
(13) Fu, Q.; Huang, S. M.; Liu, J. *J. Phys. Chem. B* **2004**, *108*, 6124−6129.
(14) Yun, S. H.; Sohn, B. H.; Jung, J. C.; Zin, W. C.; Lee, J. K.; Song, O. *Langmuir* **2005**, *21*, 6548−6552.
(15) Yoo, S. I.; Sohn, B. H.; Zin, W. C.; An, S. J.; Yi, G. C. *Chem. Commun.* **2004**, 2850−2851.
(16) Cresce, A. V.; Silverstein, J. S.; Bentley, W. E.; Kofinas, P. *Macromolecules* **2006**, *39*, 5826−5829.
(17) Cavalcanti-Adam, E. A.; Bezler, M.; Tomakidi, P.; Spatz, J. P. *J. Bone Miner. Res.* **2004**, *19*, S64−S64.
(18) Cavalcanti-Adam, E. A.; Micoulet, A.; Blummel, J.; Auernheimer, J.; Kessler, H.; Spatz, J. P. *Eur. J. Cell Biol.* **2006**, *85*, 219−224.
(19) Groll, J.; Albrecht, K.; Gasteier, P.; Riethmueller, S.; Ziener, U.; Moeller, M. *ChemBioChem* **2005**, *6*, 1782−1787.
(20) Boontongkong, Y.; Cohen, R. E. *Macromolecules* **2002**, *35*, 3647−3652.
(21) Bennett, R. D.; Miller, A. C.; Kohen, N. T.; Hammond, P. T.; Irvine, D. J.; Cohen, R. E. *Macromolecules* **2005**, *38*, 10728−10735.
(22) Bennett, R. D.; Hart, A. J.; Miller, A. C.; Hammond, P. T.; Irvine, D. J.; Cohen, R. E. *Langmuir* **2006**, *22*, 8273−8276.
(23) Bennett, R. D.; Xiong, G. Y.; Ren, Z. F.; Cohen, R. E. *Chem. Mater.* **2004**, *16*, 5589−5595.
(24) Bennett, R. D.; Hart, A. J.; Cohen, R. E. *Adv. Mater.* **2006**, *18*, 2274−2279.
(25) Cong, Y.; Zhang, Z. X.; Fu, J.; Li, J.; Han, Y. C. *Polymer* **2005**, *46*, 5377−5384.
(26) Li, X.; Tian, S. J.; Ping, Y.; Kim, D. H.; Knoll, W. *Langmuir* **2005**, *21*, 9393−9397.
(27) Zhang, G. F.; Marie, P.; Maalourn, M.; Muller, P.; Benoit, N.; Krafft, M. P. *J. Am. Chem. Soc.* **2005**, *127*, 10412−10419.
(28) Laforgue, A.; Bazuin, C. G.; Prud'homme, R. E. *Macromolecules* **2006**, *39*, 6473−6482.
(29) Xu, T.; Stevens, J.; Villa, J. A.; Goldbach, J. T.; Guarim, K. W.; Black, C. T.; Hawker, C. J.; Russell, T. R. *Adv. Funct. Mater.* **2003**, *13*, 698−702.
(30) Xu, T.; Goldbach, J. T.; Misner, M. J.; Kim, S.; Gibaud, A.; Gang, O.; Ocko, B.; Guarini, K. W.; Black, C. T.; Hawker, C. J.; Russell, T. P. *Macromolecules* **2004**, *37*, 2972−2977.
(31) Xu, C.; Fu, X. F.; Fryd, M.; Xu, S.; Wayland, B. B.; Winey, K. I.; Composto, R. J. *Nano Lett.* **2006**, *6*, 282−287.
(32) Xu, C.; Wayland, B. B.; Fryd, M.; Winey, K. I.; Composto, R. J. *Macromolecules* **2006**, *39*, 6063−6070.
(33) Shiratori, S. S.; Rubner, M. F. *Macromolecules* **2000**, *33*, 4213−4219.
(34) Katz, J. S.; Doh, J.; Irvine, D. J. *Langmuir* **2006**, *22*, 353−359.
(35) Yaffe, M. B.; Kramer, E. J. *J. Mater. Sci.* **1981**, *16*, 2130−2136.
(36) Israels, R.; Leermakers, F. A. M.; Fleer, G. J.; Zhulina, E. B. *Macromolecules* **1994**, *27*, 3249−3261.
(37) Israels, R.; Leermakers, F. A. M.; Fleer, G. J. *Macromolecules* **1994**, *27*, 3087−3093.
(38) Zhulina, E. B.; Birshtein, T. M.; Borisov, O. V. *Macromolecules* **1995**, *28*, 1491−1499.
(39) Biesheuvel, P. M. *J. Colloid Interface Sci.* **2004**, *275*, 97−106.
(40) Lyatskaya, Y. V.; Leermakers, F. A. M.; Fleer, G. J.; Zhulina, E. B.; Birshtein, T. M. *Macromolecules* **1995**, *28*, 3562−3569.
(41) Zhulina, E. B.; Borisov, O. V. *J. Chem. Phys.* **1997**, *107*, 5952−5967.
(42) Biesalski, M.; Johannsmann, D.; Ruhe, J. *J. Chem. Phys.* **2002**, *117*, 4988−4994.
(43) Currie, E. P. K.; Sieval, A. B.; Fleer, G. J.; Stuart, M. A. C. *Langmuir* **2000**, *16*, 8324−8333.
(44) Ferry, J. D. *Viscoelastic Properties of Polymers*, 3rd ed.; Wiley: New York, 1980.

MA7019418